

## Enhanced Assessment of Rainfall and Hydrologic Effects on the Triggering Mechanism of Shallow Landslides

APIP, Kaoru TAKARA, and Yosuke YAMASHIKI

### Synopsis

This study presents an approach to enhance the pioneering method for the hydrologic control on shallow landsliding. Although the previous method capable of describing combined effect of rainfall and hydrologic in triggering shallow landslides, it does not consider the effect of hydrological responses in unsaturated layer. Thus the proposed study was intended to enhance the pioneering approach. Accordingly, a coupled grid-based rainfall-runoff model and infinite slope stability approach was simplified. Linking the simplified model with the slope stability approach yields the rainfall threshold for triggering shallow landslides in saturated and unsaturated soils. Finally, coupling this model with the rainfall intensity duration frequency (IDF) can help in understanding the climate control on slope instability. This leads to predict the spatiotemporal scale of the shallow landslide occurrences. Preliminary model application is shown for the Upper Citarum River basin, Indonesia.

**Keywords:** geo-hydrologic model, unsaturated soil, rainfall threshold, shallow landslide, Citarum River.

### 1. Introduction

Flood and landslide events cause most of the major disasters in Asian countries due to socioeconomic condition and their susceptibility to these events. Although slope failures may happen due to human-induced factors such as the loading of the slope for construction purposes, landslides often occur during heavy rainfall events, especially in areas of mountainous terrain, resulting in casualties and property losses. Urgent efforts are thus needed to avoid or reduce the risk of landslides. In areas subject to fast landslides such as rapid shallow landslides, the introduction of new and innovative technology for the development of early landslide-warning systems is one of the most

effective ways to minimize damages. Therefore, shallow landslides hazard assessment and accurate estimation of rainfall-induced landslides is exactly required in landslide prediction and warning.

Landslides hazard assessment is based on a variety of approaches and models. Most rely on either multivariate correlation between mapped (observed) landslides and landscape attributes. Antecedent rainfall amounts and daily rainfall rate were further introduced as triggering factors of shallow landsliding. Up to now, the assessment of rainfall-induced shallow landslide has still been a research topic of wide concern for hydrologists and soil scientists. The empirical and statistical rainfall threshold concepts as well as the physically based model are three commonly used approaches.

The statistical approach can provide an insight of multifaceted processes involved in shallow landsliding occurrence and useful assessments of susceptibility to shallow landslide hazard in large areas. However, the results are very sensitive to the data set used in the analysis. The empirical rainfall threshold analyzed the intensity and duration of rainfalls triggering landslides. The approach built the critical rainfall threshold curves, defined as envelope curves of all rainfall triggering landslides events for a certain geographic area. Because of the lack of a process-based analysis, both methods are unable to assess the stability of a particular slope with respect to certain rainfall characteristics and they do not predict the return period of the landslide-triggering rainfall (i.e., probability of occurrence). Therefore, to investigate in more detail landslide occurrence, the physically based model needs to be used in deriving a rainfall threshold concept.

Rosso *et al.*, (2006) recently developed a physically based model for the hydrologic control on shallow landsliding. The modeling framework accounts for the variability of extreme rainfall rate and the duration. The slope stability component includes the key characteristics of the soil mantle, i.e., angle of shearing resistance, void ratio, and specific gravity of solids. Hillslope hydrology is modeled by coupling the conservation of mass of soil water with the Darcy's law used to describe seepage flow. This yields a simple analytical model capable of describing combined effect of duration and intensity of a rainfall episode in triggering shallow landslides.

Although the approach by Rosso *et al.*, (2006) capable of describing combined effect of duration and intensity of a rainfall episode in triggering shallow landslides, it does not consider the effect of hydrological responses in unsaturated layer. It only accounts the effect of rainfall role and hydrological responses in saturated layer. This simplification can affect model capability of predicting rainfall-induced shallow landslide because there had been observed that the slope failure could be caused by the loss in unsaturated shear strength when the matric suction is dissipated (Tsai *et al.*, 2008).

Thus the proposed study was intended to enhance the pioneering approach by Rosso *et al.*, (2006). Accordingly, a coupled grid-based kinematic wave rainfall-runoff model and infinite slope stability approach was simplified. The process yields relatively simple representation of dynamic hydrology –including unsaturated and saturated subsurface flows–, instead of steady state representation. Linking the simplified rainfall-runoff model with the extended Mohr–Coulomb failure criterion yields the rainfall threshold for triggering shallow landslides. The innovative aspect of the proposed method is that the produced rainfall threshold approach considers the hydrologic processes not only in non-capillary pores but also in capillary pores. Finally, coupling this model with the simple scaling model for the rainfall intensity duration frequency (IDF) can help in understanding the climate control on slope instability. This leads to predict the spatiotemporal scale of the occurrence of shallow landslides.

In the following sections, the grid-based geo-hydrologic model used for rainfall threshold method development is first described. Rainfall threshold for slope instability is then derived analytically. The effect of rainfall intensity and duration on shallow landslides in saturated and unsaturated soils is then investigated using the developed model and compares the results with the original model outputs. After a set of numerical experiments is conducted using the developed model, the applicability of new model is demonstrated in the Upper Citarum River basin, Indonesia. An analysis from coupling of the relationship between critical rainfall for different durations with the IDF curves for the return period assessment of shallow landslide occurrences at the basin scale is presented in the last section.

## 2. Geo-Hydrologic Model

A one dimensional physically based distributed hydrological model based on grid-cell kinematic wave rainfall-runoff model (Kojima and Takara, 2003) was developed for simulating hydrological responses and soil saturation. In this modelling framework, catchment topography is represented based on digital elevation model (DEM) which is divided into an orthogonal matrix of square grid-cells. A square area on a node point of a DEM is considered as a sub-catchment, which is called a grid-cell. The river catchment is modeled as a network of grid-cell. Each grid-cell receives flows from upper grid-cells and rainfall on it. These grid-cells are connected to each other with a drainage path defined by the steepest of eight-direction. Discharge and water depth diffuse to the next grid-cell according to predefined eight-direction flow map and routine order determined in accordance with DEM and river channel network data. The hillslopes flow routed and given to the river flow routing model; then the river flow is routed to the outlet.

The model simulates three lateral flow mechanisms including (1) subsurface flow through capillary pore (unsaturated flow), (2) subsurface flow through non-capillary pore (saturated flow) and (3) surface flow on the soil layer (overland flow). At each grid-cell, when the water depth is lower than the equivalent water depth  $d_m$  for the maximum volumetric water content in the unsaturated flow  $\theta_m$  ( $d_m = h^* \theta_m$ ), flow is simulated by Darcy law with degree of saturation,  $(h_w/d_m)^\beta$ , and an unsaturated hydraulic conductivity  $k_m$ . If the water depth exceeds the equivalent depth for unsaturated flow, the exceeded water flows as saturated subsurface flow that is simulated by Darcy law with saturated hydraulic conductivity  $k_a$ . Once the water depth is greater than the soil layer  $h$  times effective porosity  $\theta_a$  ( $d_a = h^* \theta_a$ ), the water flows as surface flow, which is simulated by the Manning's equation. Herein, the basic assumption that the flow lines are parallel to the slope and the hydraulic gradient is equal to the slope. In addition, the kinematic wave

model assumes that rainfall intensity always lower than infiltration rate capacity. Thus it does not consider the vertical water flow, the input rainfall data is directly added to subsurface flow or surface flow according to the water depth on the area where the rainfall dropped. Regarding this mechanism, overland flow happens if the depth of water exceeds the soil water capacity. Details on the derivation of this model equations are given by Sayama and McDonnell (2009).

These processes are represented with a kinematic wave model using function for the stage-discharge relationship. An advantage of the model is that the stage-discharge relationship of each grid-cell reflects the topographic and physical characteristics (i.e., land use and soil type) of its own grid. These three flow processes are represented by the following single set of stage-discharge relationship (Tachikawa *et al.* 2004):

$$q = \begin{cases} v_m d_m (h_w / d_m)^\beta, & 0 \leq h_w \leq d_m \\ v_m d_m + v_a (h_w - d_m), & d_m < h_w \leq d_a \\ v_m d_m + v_a (h_w - d_m) + \alpha (h_w - d_a)^k, & d_a < h_w \end{cases} \quad (1)$$

$$v_m = k_m i, \quad v_a = k_a i, \quad k_m = k_a / \beta, \quad \alpha = \sqrt{i} / n,$$

where  $q$  is discharge per unit width,  $h_w$  is water depth,  $i$  is the topography gradient,  $k_m$  is the saturated hydraulic conductivity of the capillary soil layer,  $k_a$  is the hydraulic conductivity of the non-capillary soil layer,  $d_m$  is the depth of the capillary soil layer,  $d_a$  represents the depths of the capillary and non-capillary soil layers,  $\beta$  is the exponent constant of unsaturated flow ( $= 2$ ),  $v_m$  and  $v_a$  are the flow velocities of unsaturated and saturated subsurface flows, respectively,  $n$  is the Manning's roughness coefficient varies as a function of land use type, and  $k$  is a constant ( $= 5/3$ ).

The slope stability model is developed based on the concept of the infinite slope model, using the factor of safety (FS) that considers a failure surface. The following are assumed: (i) failure is the result of translation sliding, (ii) the failure plane and water table are parallel to the ground surface, (iii) failure

occurs as a single layer, (iv) the failure plane is of infinite length, and (v) the impacts of adjacent factors are not taken into account. For hillslopes, the safety factor generally is represented as the ratio of the available resisting force (shear strength) to the driving force (shear stress). Instability occurs when the shear strength of a soil layer becomes smaller than the shear stress acting on the soil. The governing equation of the safety factor used in this study is based on a Mohr–Coulomb failure law.

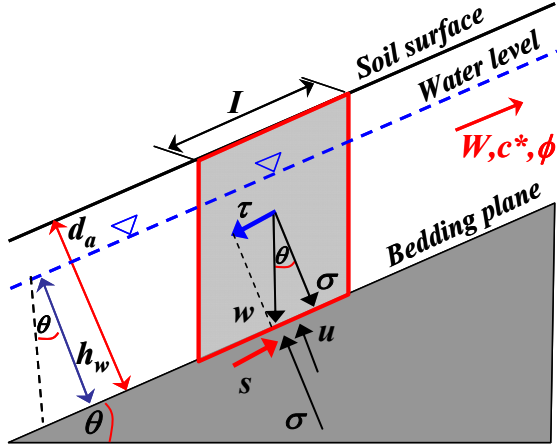


Fig. 1 Forces diagram on a slice of an infinite slope.

Figure 1 illustrates the forces acting on a point along a slope with potential for failure. The resisting force of a soil layer is the shear strength ( $s$ ) as a combination of forces, including the normal stress ( $\sigma$ ), pore pressure ( $u$ ) within the soil material, cohesion factors ( $c$ ), and the effective angle of internal friction in degrees ( $\phi$ ). The resultant force between normal stress and pore pressure is the effective normal stress. Shear strength based on the Mohr–Coulomb law can be expressed as follows:

$$s = c + (\sigma - u) \tan \phi \quad (2)$$

Normal stress is the vertical component of gravity that resists downslope movement as follows:

$$\sigma = \rho_s g \cos \theta d_a + W \cos \theta, \quad (3)$$

where  $\rho_s$  is the wet soil density ( $\text{kg/m}^3$ ),  $g$  is the gravitational acceleration ( $= 9.81 \text{ m/s}^2$ ),  $d_a$  is the vertical soil depth perpendicular to the slope (m),  $W$  is the vegetation surcharge ( $\text{N/m}^2$ ), and  $\theta$  is the slope angle (deg). Soil moisture increases the unit weight

of soil material; therefore it increases both the resisting and driving forces. Soil moisture creates pore pressure, which reduces the effective normal stress and shear strength. Pore pressure in the slope differs among sites and also has large temporal variation. It is difficult to estimate these values and to include them in this model of a large basin. Therefore, we simplified the condition of pore pressure in the slope by assuming that the pore pressure in the slope is always in the static state condition. Pore pressure is quantified by the following equation when assuming no excess pore water pressure:

$$u = \rho_w g h_w \cos \theta, \quad (4)$$

where  $\rho_w$  is the density of water ( $= 1000 \text{ kg/m}^3$ ) and  $h_w$  is the height of the water depth perpendicular to the slope (m). This assumption gives greater pore water pressure in the rising process of the subsurface water and smaller pore water pressure in the descending process of the subsurface water.

The shear stress as driving force, defined by the downslope parallel component of gravity, can be expressed as follows:

$$\tau = \rho_s g \sin \theta d_a + W \sin \theta \quad (5)$$

By substituting the formula for shear strength and shear stress, the factor of safety is calculated as follows

$$FS = \frac{c^* + \cos \theta [1 - r_w] \tan \phi}{\sin \theta}, \quad \begin{cases} c^* = \frac{c_r + c_s}{d_a \rho_s g + W} \\ r_w = \frac{h_w \rho_w}{\left(1 + \frac{W}{g d_a \rho_s}\right) d_a \rho_s} \end{cases} \quad (6)$$

in which  $c^*$  is the total cohesion ( $c_r + c_s$ ),  $c_r$  and  $c_s$  is the effective root and soil cohesion ( $\text{N/m}^2$ ). The dimensionless form of Equation (6) has been widely used to analyse the stability of shallow soil using digital terrain models.

According to Equation (6), most of the variables could be set up as spatially distributed, but it is assumed that only  $h_w$  is time-varying. The water

depth,  $h_w$ , is determined by the flux of subsurface water flow computed by the hydrological model (see Equation 1). Here the ratio ( $m = h_w/d_a$ ) shows that the relative saturated depth is time-dependent (range numerically between 0.0 and 1.0). Whenever  $FS < 1.0$ , the driving forces prevail, and the potential for failure is high. Through an inversion of the standard factor of safety (Equation 6), a fixed time-invariant critical relative soil saturation ( $m^c$ ) triggering slope instability (i.e., relative soil saturation that yields  $FS = 1.0$ ) for each grid element could be approximated as

$$m^c = \left( \frac{\rho_s}{\rho_w} + \frac{W}{gd_a\rho_w} \right) \left( 1 - \frac{\tan\theta}{\tan\phi} \right) + \frac{c_r + c_s}{d_a\rho_w g \cos\theta \tan\phi} \quad (7)$$

Based on the concept of critical relative soil saturation, three slope stability classes could be defined as theoretically “stable”, potentially “stable/unstable”, and theoretically “unstable” (Montgomery and Dietrich 1994). The theoretically “**stable**” condition refers to those slopes that are stable even when saturated soil depth reaches the ground surface,  $m^c = 1.0$ . Similarly, slopes that are predicted to be unstable even under a dry condition (i.e.,  $m = 0.0$ ) are considered to be theoretically “**unstable**”; such slopes affected by suction force or composed of rocks. In the unsaturated soil layer, suction (negative pore water pressure) is working and provides additional shear strength. This force is also difficult to include in the model at present. In addition, there is no subsurface flow processes for the slope elements where the soil mantle spaces composed by the impermeable bedrock. Therefore, we excluded the slope areas characterized as theoretically “**unstable**” from the target of this research.

In this study, the critical relative soil saturation depth obtained by Equation (7) and time-dependent slope instability analysis were calculated only for those grids with slope stability classified as potentially “**stable/unstable**”; these grids were defined as the target area for simulating slope instability as a function of time.

### 3. Derivation of Rainfall and Hydrologic Thresholds Triggering Mechanism of Slope Instability Considering Unsaturated and Saturated Subsurface Flows

The fundamental assumption of the lumping kinematic wave rainfall-sediment-runoff method (Apip *et al.*, 2008) is adopted. Thus discharge flux can be expressed as the product of rainfall intensity and the drainage area with spatially uniform rainfall input. Applying conservation of mass to the Equation 1 yield a general equation as follows

$$Ar - wq = \frac{ds}{dt} = A \frac{dh_w}{dt} \quad (8)$$

with  $A$  is the upslope contributing area draining across  $w$ ;  $w$  is the width of grid at the lower bound;  $r$  is the rainfall;  $s$  is the water storage;  $t$  is the time after the beginning of the rainfall;  $q$  is the water discharge per unit width; and  $h_w$  is the water height. By substituting the  $q$  equations for unsaturated and saturated flows (see Equations 1) to Equation 8, and integrating the differential equation for the initial condition of  $h_w(0) = h_i$ ,  $h_w$  for a rainfall with duration  $t$ ,  $h_{w-t}$  can be yielded depending on the soil saturation condition and  $q$ - $h_w$  relationships for sub-surface layer as follows:

For the case of unsaturated flow with the parameter  $\beta = 2$

$$h_{w-t} = \frac{\left( \exp\left(\frac{2t\sqrt{v_m w A r}}{A\sqrt{d_m}}\right) x \left( \frac{\sqrt{d_m r A} + h_i \sqrt{v_m w}}{h_i \sqrt{v_m w} - \sqrt{d_m r A}} \right) x (h_{w-t} \sqrt{v_m w} - \sqrt{d_m r A}) \right) - \sqrt{d_m r A}}{\sqrt{v_m w}} \quad (9)$$

For the case of saturated flow

$$h_{w-t} = \frac{\left( \frac{r}{w} A - d_m (v_m - v_a) \right)}{v_a} \left( 1 - \exp\left(\frac{-wv_a t}{A}\right) \right) + h_i \exp\left(\frac{-wv_a t}{A}\right) \quad (10)$$

Figure 2 shows the variability of  $h_w$  and discharge  $Q$ , respectively, with rainfall duration  $t$  for different values of  $w$ . For given slope, soil thickness, hydraulic conductivity, initial condition, drainage area, and net rainfall rate, an increase of the  $w$  yields the steady state thickness of the subsurface water height

to decrease. The rate of increase of  $h_w$  in time is much higher for small  $w$  than those characterizing large values of  $w$ . Thus large values of  $w$  yield water production to rapidly achieve steady state conditions, while much more time is needed for elementary areas with small values of  $w$  to achieve steady state runoff production. For the same rainfall condition, the value of  $w$  determines the position to reach a steady state condition. Figure 3 presents the relationship between dynamic hydrological responses and the factor of safety

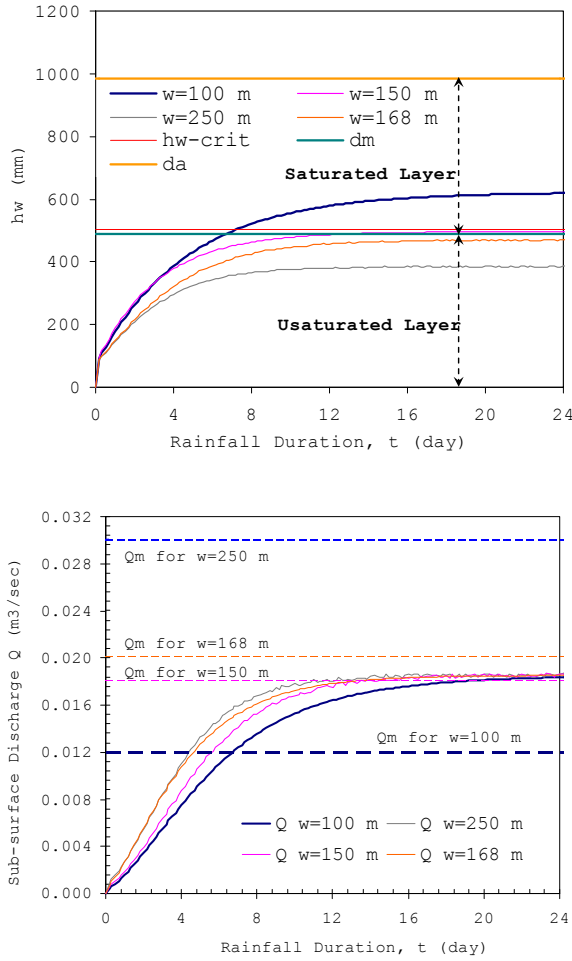


Fig. 2 Height of the water table (upper figure) and water discharge production (lower figure) versus rainfall duration for different  $w$  under specified conditions ( $r = 80$  mm/day,  $k_a = 80000$  mm/day,  $D = 1477.11$  mm,  $d_a = 0.667 * D$ ,  $d_m = 0.331 * D$ ,  $i = 32$  degree, initial condition of water depth =  $0.15 d_m$ ).  $d_m$  is the maximum capillary layer depth;  $d_a$  is the non-capillary layer depth;  $Q_m$  is the maximum subsurface discharge for unsaturated flow.

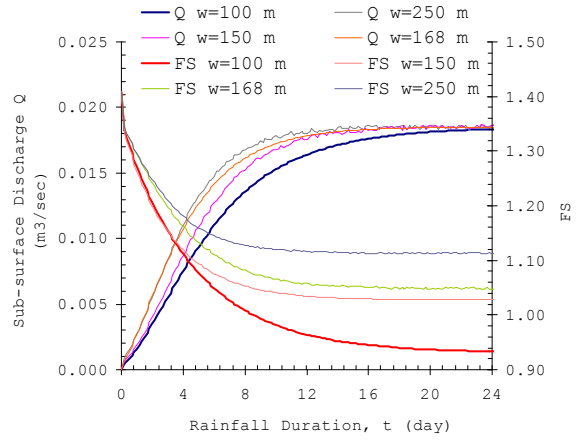


Fig. 3 Rainfall duration versus subsurface water discharge and flux of safety factor FS for different  $w$  under specified conditions ( $r = 80$  mm/day,  $k_a = 80000$  mm/day,  $D = 1477.11$  mm,  $d_a = 0.667 * D$ ,  $d_m = 0.331 * D$ ,  $i = 32$  degree, initial condition of water depth =  $0.15 d_m$ ).

Coupling hillslope hydrology with infinite slope stability approach yields shallow landslide triggering by rainfall. This is obtained by substituting the right-hand side of Equation 9 or 10 to the equation of critical saturated depth (Equation 7). Solving the above equation obtains the rainfall rate threshold,  $r_c$ , causing instability in the unsaturated and saturated zones as follows

For the case of unsaturated flow with the parameter  $\beta = 2$

$$r_c = \frac{B^2}{d_m A} \quad (11)$$

where  $B$  is expressed as

$$\sqrt{v_m w} \left( \left( \frac{d_a \rho_s}{\rho_w} + \frac{W}{g \rho_w} \right) \left( 1 - \frac{\tan \theta}{\tan \phi} \right) + \frac{c_s + c_r}{\rho_w g \cos \theta \tan \phi} \right) + \left( \exp \left( \frac{2t \sqrt{v_m w A r}}{A \sqrt{d_m}} \right) x \frac{\sqrt{d_m r A} + h_i \sqrt{v_m w}}{h_i \sqrt{v_m w} - \sqrt{d_m r A}} x (h_{w-t} \sqrt{v_m w} - \sqrt{d_m r A}) \right)$$

For the case of saturated flow

$$r_c = \frac{w v_a \left( \left( \frac{d_a \rho_s}{\rho_w} + \frac{W}{g \rho_w} \right) \left( 1 - \frac{\tan \theta}{\tan \phi} \right) + \frac{c_s + c_r}{\rho_w g \cos \theta \tan \phi} - h_i \exp \left( \frac{-w v_a t}{A} \right) \right)}{\left( 1 - \exp \left( \frac{-w v_a t}{A} \right) \right) A} +$$

$$\frac{wd_m(v_m - v_a)\left(1 - \exp\left(\frac{-wv_a t}{A}\right)\right)}{\left(1 - \exp\left(\frac{-wv_a t}{A}\right)\right)A} \quad (12)$$

The intensity-duration-frequency relationship (IDF) for station rainfall provides the probability that a given rainfall intensity is exceeded over a specified duration of the rainfall. Thus coupling of the model for the hydrologic control on shallow landsliding with the simple scaling model for the frequency of storm precipitation can help understanding the climate control on landscape development associated with the occurrence of shallow landslides

### Numerical Experiments

The below figures illustrate a comparison between the proposed method (unsaturated and saturated zones) with the original method (saturated zone) by Rosso using average input rainfall  $r = 80$  mm/day with different duration.

#### Hydrology and Slope Instability

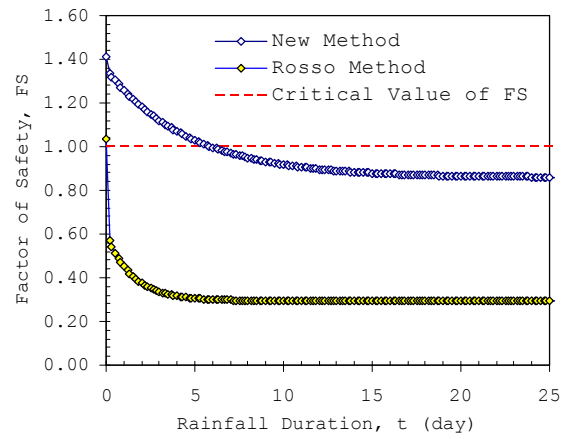
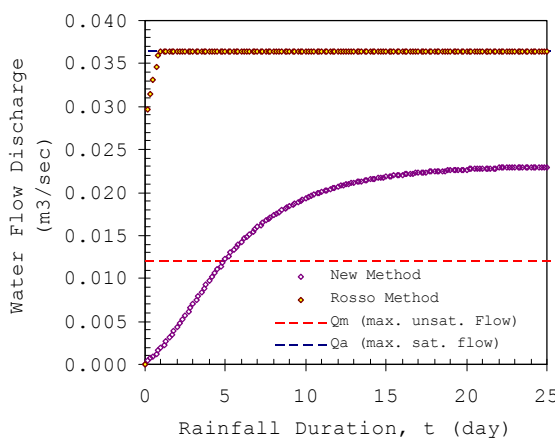
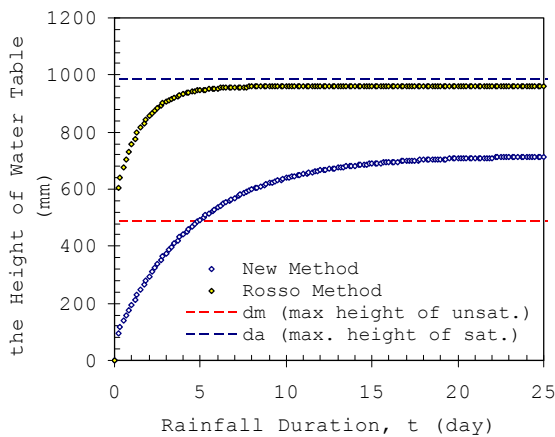


Fig. 4 Hydrologic responses and its slope stability condition for different rainfall duration computed using new method and the original one.

#### Rainfall Threshold

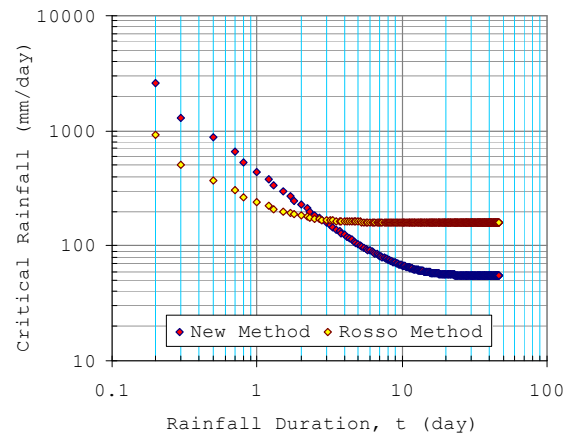


Fig. 5 The comparisons of predicted rainfall threshold for different rainfall duration role computed by the new method and the original approach.

## 4. Model Application

### Study Area

The Upper Citarum River basin with Saguling Reservoir as the outlet was selected for the preliminary model application. This study region is located in mountainous area of the West Java Province, and total area of the upper basin is the 2,310 km<sup>2</sup> lying between 600 to 3000 m. Geographically, the area is lies off 107°26'E-107°95'E and 6°73'S-7°25'S. The average of slope gradients by using a DEM 90 m resolution

range from  $0.01^\circ$  in the central area to  $31.15^\circ$  in northern and southern parts.

The current water related problems are floods and landslides in the wet season and droughts in the dry season. The hillslopes areas of this region have been periodically exposed to hazards from shallow landslides and debris flows. Most of those landslides were triggered by a series heavy rainfall. The climate conditions are characterized by tropical monsoon with two distinct wet and dry seasons. A series of data from BMG specifying that high amount of rainfall is at the beginning of November-December followed by a second peak in March-April, results from the westerly monsoon. The rainfall amount then quickly slackening down in May-October due to dry season as results from the prevailing easterly monsoon. Annually rainfall of the area varies from 1500 mm up to 4000 mm, with almost 80% falling between November and April.

Annual maximum rainfall series were supplied from one automatic rain gauge in the upper Citarum catchment, namely at BMG Station. As result of a frequency analysis, GEV distribution was selected as the best fit probability distribution. Figure 6 shows the IDF curves for the Upper Citarum River basin.

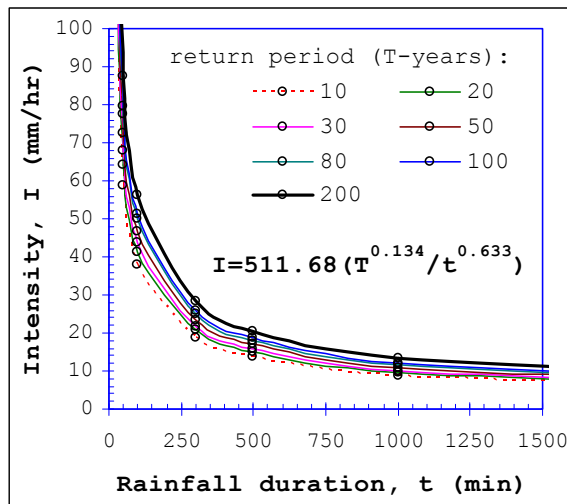


Fig. 6 IDF Curves for the Upper Citarum River basin, Indonesia.

### Coupling of the relationship between critical rainfall with the IDF curves for the failure return period under specified slope grid

The example of Figure 7 shows that the topographic condition ( $w$ ) strongly controls the return period of expected hillslope instability, but is also has a not negligible influence on the critical duration of rainfall triggering shallow landslides. It is seen that increasing of ( $w$ ) yields the return period of potential failure to increase, and the critical duration of precipitation for hillslope instability to increase. In fact for  $w = 100$  the return period of potential failure is ten years for the critical rainfall duration of about eight days, while for  $w = 250$  the return period of potential failure is more than 200 years for the critical rainfall duration of about one eight days. Other factors related to the soil properties and initial soil moisture condition also strongly controls the return period of expected hillslope instability as illustrated in Figures 8-10.

### Rainfall Threshold for Slope Instability under Specified Conditions

#### Control

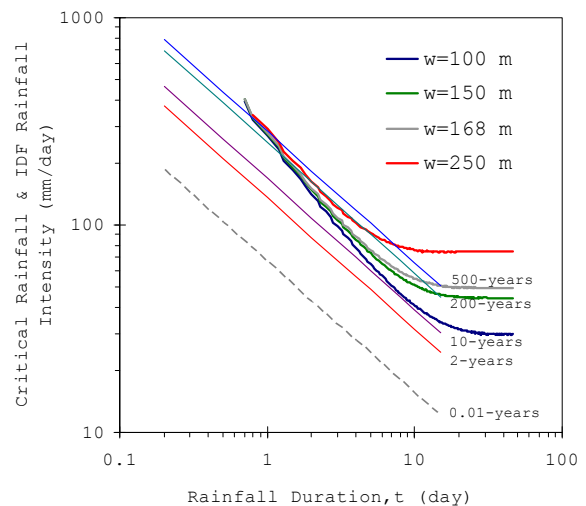


Fig 7. Coupling of the relationship between critical rainfall rate and duration of rainfall with the IDF curves for the failure return period under specified condition:  $k_a=80000$  mm/day,  $D=1200$  mm,  $\theta_a=0.667$ ,  $\theta_m=0.331$ , slope=36,  $\text{fric}=42$ ,  $C=400$  N/m<sup>2</sup>,  $V_{eg}=200$  N/m<sup>2</sup>,  $I_{init}=0.15$  dm.



*Effect of initial soil saturation*

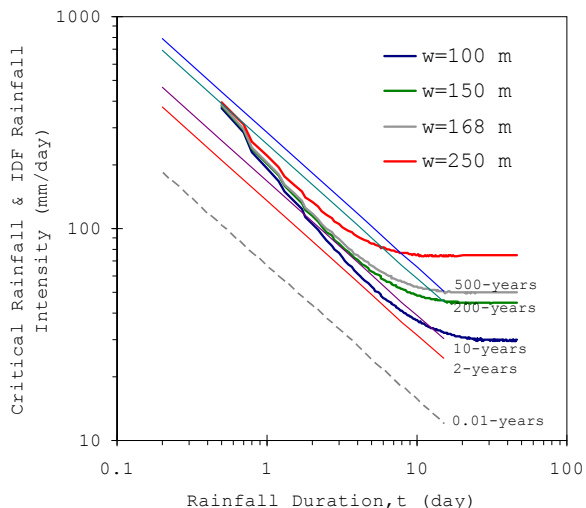


Fig 8. Coupling of the relationship between critical rainfall rate and duration of rainfall with the IDF curves for the failure return period under specified condition:  $k_a=80000$  mm/day,  $D=1200$  mm,  $\theta_a=0.667$ ,  $\theta_m=0.331$ , slope=36, fric=42,  $C=400$  N/m<sup>2</sup>, Veg=200 N/m<sup>2</sup>,  $I_{init}=0.15$  dm

*Effect of slope angle*

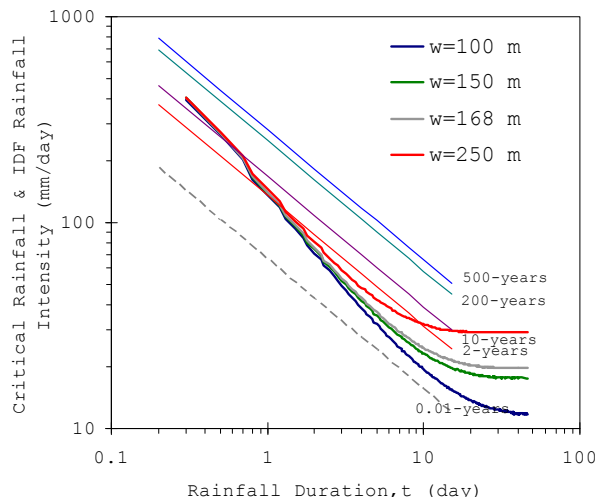


Fig 10. Coupling of the relationship between critical rainfall rate and duration of rainfall with the IDF curves for the failure return period under specified condition:  $k_a=80000$  mm/day,  $D=1200$  mm,  $\theta_a=0.667$ ,  $\theta_m=0.331$ , **slope=40**, fric=42,  $C=400$  N/m<sup>2</sup>, Veg=200 N/m<sup>2</sup>,  $I_{init}=0.15$  dm.

*Effect of change in saturated hydraulic conductivity*

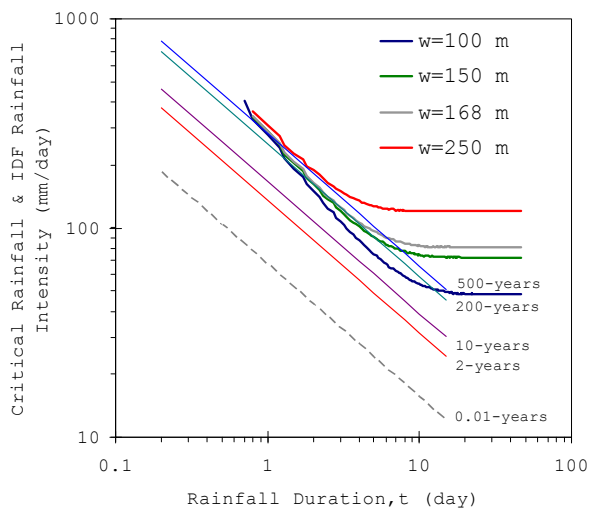
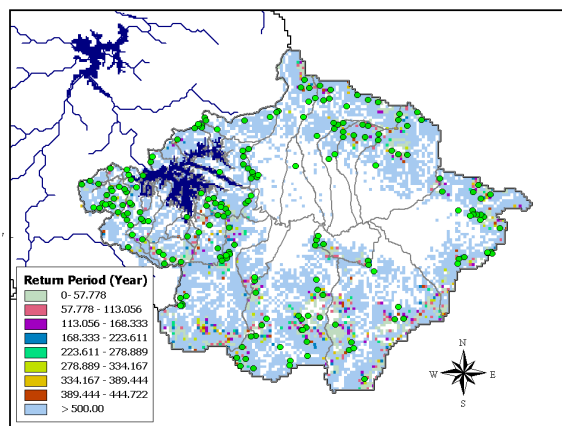


Fig 9. Coupling of the relationship between critical rainfall rate and duration of rainfall with the IDF curves for the failure return period under specified condition:  **$k_a=120000$**  mm/day,  $D=1200$  mm,  $\theta_a=0.667$ ,  $\theta_m=0.331$ , slope=36, fric=42,  $C=400$  N/m<sup>2</sup>, Veg=200 N/m<sup>2</sup>,  $I_{init}=0.15$  dm

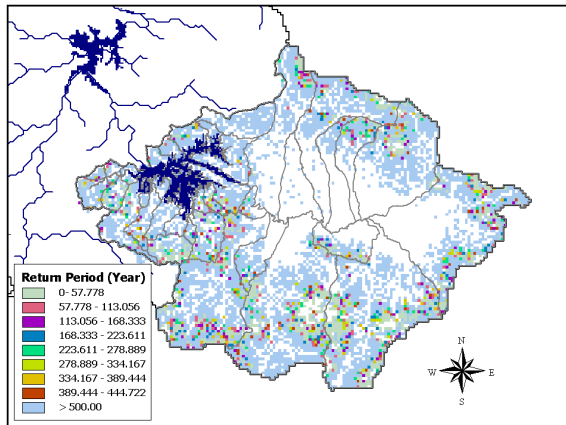
**Return Period of Potential Slope Failure for  $r=50$  mm/day**

Model application in predictive mode is carried out for the Upper Citarum River basin in Indonesia. The IDF curves for this site are estimated from 22 years of station rainfall data recorded at Bandung City, using the GEV distribution (see Figure 6). Figure 11 shows the resulting map of the Upper Citarum River basin where the return period of rainfall causing potential failure is reported considering different set of rainfall duration.

*3 days duration*



6 days duration



12 days duration

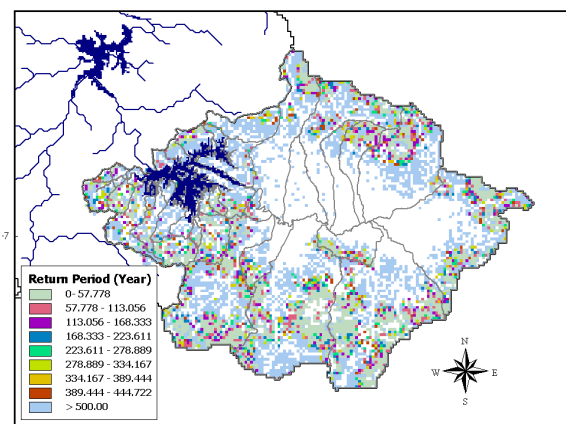


Fig 11. Map of the Upper Citarum River basin showing shallow landsliding prone areas as predicted from the application of the present model in terms of return period of potential failure under different set of rainfall duration.

## Conclusions

An enhanced approach was developed here to improve the representation of soil properties and hillslope hydrology in the pioneering model by Rosso *et al.*, (2006) of shallow landslide initiation.

The approach yields a simple runoff production triggering slope instability model, capable of properly

accounting for topography, soil transmissivity, and initial soil moisture in capillary pores (unsaturated flow) and non-capillary pores (saturated flow) that were missed in the steady state approach by Rosso *et al.*, (2006). The model can describe transient rainfall and the threshold effect associated with the achievement of saturation of the soil mantle.

## References

- Apip, Sayama, T., Tachikawa, Y. and Takara, K. (2008): Lumping of a physically-based distributed model for sediment runoff prediction in a catchment scale, *Annual Journal of Hydraulic Engineering, JSCE*, Vol. 52, pp 43-48.
- Montgomery, D.R., and Dietrich, W.E. (1994): A physically-based model for the topographic control on shallow landsliding. *Water Resources Research*, Vol. 30, pp. 1153-1171.
- Rosso, R., Rulli, M.C., and Vannuchi, G. (2006): A physically based model for the hydrologic control on shallow landsliding. *Water Resources Research*, 42, W06410: pp. 1-16.
- Sayama, T., and McDonnel, J.J. (2009): A new time-space accounting scheme to predict stream water residence time and hydrograph source components at the watershed scale. *Water Resources Research*, 45: pp. 1-14
- Tachikawa, Y., Nagatani, G., and Takara, K. (2004): Development of stage-discharge relationship equation incorporating saturated-unsaturated flow mechanism. *Annual Journal of Hydraulic Engineering (JSCE)*, pp 48: 7-12.
- Tsai, T.L., Chen, H.E., and Yang, J.C. (2008): Numerical modeling of rainstorm-induced shallow landslides in saturated and unsaturated soils. *Environ Geol*, Vol., 55: pp. 1269-1277.

# 浅層地滑り発生機構解明における降水と水文過程の影響評価について

APIP・宝 馨・山敷庸亮

## 要 旨

本研究は浅層地滑りに対する画期的な水文学的制御方法について述べる。以前の研究で提案した方法において地滑り発生における降雨の継続時間や水文学的影響を評価したが、不飽和層の水文学的応答については考慮していなかった。そのため本研究においては革新的手法、すなわちセルに適用する特性曲線法を用いた降雨流出モデルや斜面安定解析などが簡便化された方法を用いている。この簡便化した降雨流出解析を斜面安定解析に結びつける事により飽和／不飽和土層の浅層崩壊の閾値を定める事が可能となる。最終的にこのモデルを降雨強度・継続時間・頻度に関する単純な相似モデルと組み合わせることにより斜面崩壊における気候の要因があきらかになる。最終的に浅層崩壊の発生を時間空間的に予測することができ、このモデルのインドネシア／チタラム川流域への適用を行なった。

**キーワード:** 地質学水文学モデル, 不飽和土層, 降雨閾値, 浅層崩壊, チタラム川流域